


Microstructure and Magnetic Properties of Exchange-Coupled $\text{Co}_{72}\text{Pt}_{28}/\text{Pt}/\text{Co}_{81}\text{Ir}_{19}$ Composite Media for Perpendicular Magnetic Recording

Z. W. Li¹  · J. Y. Jiao¹ · Z. Luo¹ · T. Y. Ma¹ · L. Qiao¹ · Y. Wang¹ · T. Wang¹ · F. S. Li¹

Received: 29 October 2018 / Accepted: 21 November 2018 / Published online: 15 January 2019
© Springer Science+Business Media, LLC, part of Springer Nature 2018

Abstract

In this work, we report the investigation of microstructure and magnetic properties of the $\text{Co}_{72}\text{Pt}_{28}/\text{Pt}/\text{Co}_{81}\text{Ir}_{19}$ exchange-coupled composite (ECC) media using soft-layer (SL) of $\text{Co}_{81}\text{Ir}_{19}$ with negative magnetocrystalline anisotropy (MA). Our TEM images show that the hard-layer (HL) exhibits a columnar type microstructure with well-isolated grains and the exchange-coupled SL with *hcp*-structure show the same texture. Strong coupling of the two layers have been evidenced by the magnetic characterization for all the studied films with Pt inter-layer thickness ranging from 0 to 2 nm. Importantly, these ECC media films have much lower coercivities and much higher thermal stabilities in the favor of high-density magnetic recording.

Keywords Magnetic thin film · Negative magnetocrystalline anisotropy · ECC media

1 Introduction

To further increase the areal density in magnetic recording, materials with large magnetocrystalline anisotropy (MA) were used to increase the superparamagnetic limit (energy barrier $\Delta E = KV$). However, this will results in an unfavorable increase of the coercivity, and then in an increased writability which was limited by the maximum fields achievable with the current writing heads to about 1.7 T [1]. Different approaches such as exchange-coupled composite (ECC) media [2–5] and heat/microwave/light-assisted magnetic recording [6–8] have been used to reduce the coercivity of the recording media with very high uniaxial anisotropy. Among these methods, the magnetically coupled ECC media with hard/soft multi-layer structure, have

attracted much attention due to their promising potential in resolving the abovementioned problem [2–5].

Theoretically, many work have been performed to study the effects of soft-layer (SL) thickness [9, 10], anisotropy constant [11–13], hard/soft layer coupling strength [4, 14–16], and the magnetization reversal process [15, 17, 18] of the ECC media. Following these work, many experiments have been done using FePt [19–24], CoPt [25–29] as the hard layer (HL) due to their high uniaxial MA which is essential to maintain high thermal stability. Considerable reduction of the coercivity has been achieved by changing the SL composition [22, 25, 26] which changes the MA constant, and by changing the SL and/or interlayer thickness [19–21, 27–29] which optimizes the coupling strength of hard/soft layers, thus improving the writability of the recording media while maintaining high thermal stability.

Following the theoretical work of Suess et al. [12], most of these experiments were done using SLs with positive but negligible MA, $K_s \sim 0$. However, as shown in our previous work [30], the theoretical model proposed by Victora et al. [31] is more adequate to describe the ECC system. By using this model, Wang et al. [13] have shown that negative SL anisotropy actually has a beneficial contribution in decreasing the switching field. In our earlier work [30], a series of samples with different SL thicknesses and

✉ Z. W. Li
zweili@lzu.edu.cn

T. Wang
wtao@lzu.edu.cn

¹ Key Lab for Magnetism and Magnetic Materials of the MOE, Key Lab for Special Functional Materials and Structure Design of the MOE, Lanzhou University, Lanzhou, 730000, People's Republic of China

composition have been studied which shows that negative SL MA is more efficient in reducing the coercivity of the ECC media in good accordance with the theoretical prediction of Victora et al. [13, 31]. Negative MA were realized by changing the Ir content of the $\text{Co}_{100-x}\text{Ir}_x$ SL. By oriented-growth of the *hcp*- $\text{Co}_{81}\text{Ir}_{19}$ (negative MA with $x = 19$) layer with its crystallographic *c*-axis parallel to the normal of the film surface, its magnetic moments can be restricted strictly in-plane by its very strong negative total in-plane anisotropy of our ECC films [30, 32, 33].

To better improve our understanding of this system, in this work, we further investigated the microstructure and magnetic properties of the exchanged-coupled $\text{Co}_{72}\text{Pt}_{28}/\text{Pt}(t\text{ nm})/\text{Co}_{81}\text{Ir}_{19}$ with different Pt inter-layer thicknesses, $t = 0 \sim 2$ nm. Our results show that, when compared with uncoupled system, these ECC media films have much lower coercivities and much higher thermal stabilities, which is very promising in high density perpendicular magnetic recording.

2 Experiments

The investigated $\text{Co}_{72}\text{Pt}_{28}/\text{Pt}/\text{Co}_{81}\text{Ir}_{19}$ ECC media were prepared by perpendicular DC magnetron sputtering technique with a layered structure of substrate/Ta(5 nm)/Pt(10 nm)/Ru(15 nm)/ $\text{Co}_{72}\text{Pt}_{28}$ (20 nm)/Pt(t nm)/ $\text{Co}_{81}\text{Ir}_{19}$ (4 nm) with $t = 0 \sim 2$ nm (see Fig. 1). For simplicity, our sample will be denoted as Pt(t) where Pt represents the Pt inter-layer and $t = 0, 0.5, 1.0, 1.5, 2.0$ stands for the thickness of this layer. For the substrate, Si(100)-orientation wafer with surface oxidation was used. On top of the substrate, Ta(5 nm) amorphous layer was grown to provide a flat and clean surface. Then, Pt(10 nm) layer with (111) orientation was grown to promote Ru(002) texture of the seed layer which

will induce the columnar growth of the $\text{Co}_{72}\text{Pt}_{28}$ HL with well-isolated grains [30, 34, 35]. For the growth of the HL and SL, Ar pressures of 4 Pa and 0.3 Pa were used, respectively. The base pressure before deposition was lower than 2×10^{-5} Pa.

Chemical composition of our thin films have been characterized by energy dispersive spectrometer. Grain morphology of the sample was measured using a transmission electron microscope (TEM). The crystal structure of our sample was checked by x-ray diffraction (XRD) with Cu $K_{\alpha 1}$ radiation. Characterization of the magnetic properties were done with a vibrating sample magnetometer (VSM). Dynamic magnetic properties were measured with an electron spin resonance spectrometer (ESR) to determine the intrinsic MA constant and the detailed procedure can be found in our previously published works [32, 33]. These measurements were all done at room temperature and our samples were stored under vacuum except the measurement procedures.

3 Results and Discussion

Figure 1 presents typical TEM images of the cross section of sample Pt(2.0). Columnar type growth of the $\text{Co}_{72}\text{Pt}_{28}$ layer with well-isolated grains can be seen from the image shown in Fig. 1a and the well-isolated nature of these grains are also reflected by the tilted magnetic hysteresis loop of the single HL sample as shown later in Fig. 3 [30, 35]. From the enlarged view shown in Fig. 1b, one can see the parallel orientation of the *c*-plane of the *hcp*-type HL and SL which was induced by the perfect orientation of the seed layer as shown in Fig. 1c.

The XRD patterns of our samples are shown in Fig. 2. All samples exhibit three main peaks at 39.6° , 42.1° ,

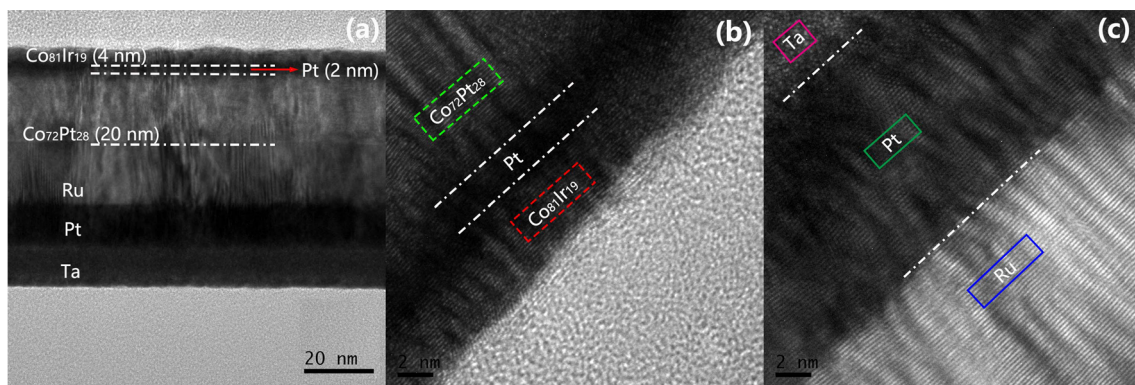


Fig. 1 (Color online) TEM images of the cross section of the Pt(2.0) sample: **a** cross section of the entire film showing the layered structure of our ECC media, **b** enlarged view of the ECC media layer, and **c** enlarged view of the seed layer

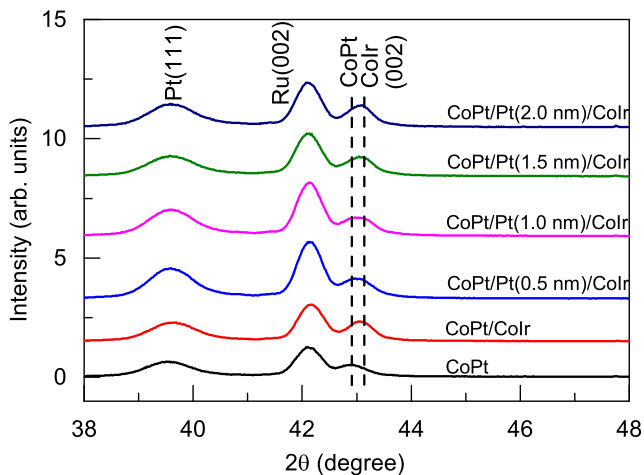


Fig. 2 (Color online) XRD patterns of the investigated samples with indicated Pt inter-layer thicknesses. The two vertical dashed lines represent peak positions corresponding to the (002) planes of the HL and SL. Patterns for pure HL sample and sample with no Pt inter-layer were also shown

and $\sim 43.1^\circ$ which correspond to Pt (111), Ru (002), and $\text{Co}_{72}\text{Pt}_{28}/\text{Co}_{81}\text{Ir}_{19}$ (002) peaks [34, 36], respectively. Similar to our earlier work [30], closer check on the third peak at 43° , one can find that the peak is actually composed of two peaks corresponding to the HL ($\text{Co}_{72}\text{Pt}_{28}$) and SL ($\text{Co}_{81}\text{Ir}_{19}$) as indicated by the two vertical dashed lines in Fig. 2. These results prove the successful growth of our ECC films. Importantly, the only observable (002) peak for the HL and SL layers indicate the perfect oriented-growth of the these layers, which is consistent with our TEM results shown above. Therefore, since the HL (SL) layer exhibit positive (negative) MA, the easy magnetic direction of the HL (SL) layer is then parallel (perpendicular) to the surface normal of our ECC film [30, 32, 34, 36].

Normalized magnetic hysteresis loops of our sample were shown in Fig. 3. As reported in our earlier work, the easy-axis coercivity and saturation magnetization were determined to be 0.51 T and 1.1×10^6 A/m, respectively. The MA of the HL amounts to 1.25×10^6 J/m³ as calculated by the area difference between the hard-axis and easy-axis hysteresis loops [30]. These magnetic parameters are very close to reported values of similar composition [34, 37]. One can see that the hysteresis loops are not vertical at the magnetization reversal region (close to the coercivity part), indicating weak inter-granular coupling of the HL, which is favorable for actual application in perpendicular magnetic recording [35].

Interestingly, when compared to the single HL film, the coercivity of the ECC media films were greatly reduced. However, with the insertion of the Pt inter-layer, the coercivity of the films increase a little bit as summarized in

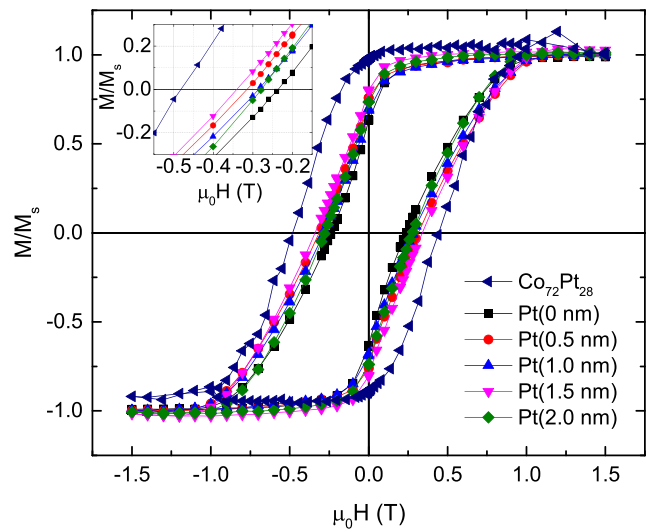


Fig. 3 (Color online) Magnetic hysteresis loops of the pure HL film and ECC films with Pt inter-layer thicknesses ranging from 0 to 2.0 nm grown on the same seed-layer measured with applied magnetic field along the surface normal of the films

Fig. 4 for a clear view. But, one can see that it is still much lower than that of the pure HL film which is helpful for improving the writability of the recording media. Another interesting feature is that no obvious steps were observed during the magnetization reversal process for all these ECC media films, indicating strong coupling between the hard and soft layers despite the Pt inter-layer between the two layers.

To better understand the trend of the coercivity changing, we would like to turn to the theoretical model used in our earlier work [30]. As already discussed, our data can be better explained using the model proposed by Victora et al.

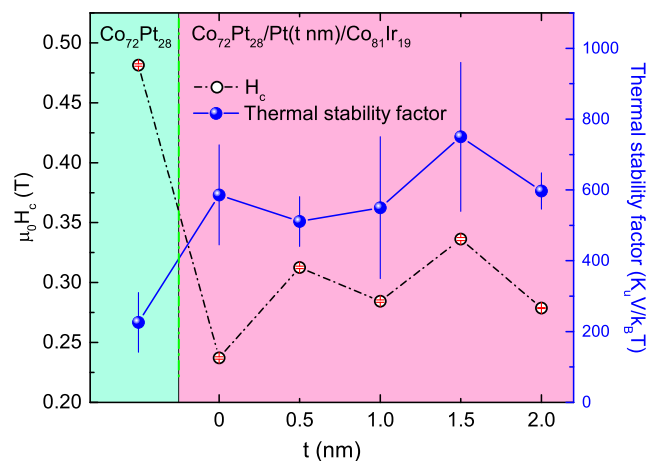


Fig. 4 (Color online) Pt inter-layer thickness dependence of the coercivity (left axis) determined from the VSM measurements and thermal stability factor (right axis) of our pure HL film and ECC films

where the total magnetic energy of the ECC system can be expressed by [31]

$$E = HM_1\cos\theta_1 V_1 + HM_2\cos\theta_2 V_2 + K_1\sin^2\theta_1 V_1 + K_2\sin^2\theta_2 V_2 - J_e\cos(\theta_1 - \theta_2). \quad (1)$$

$\mu_0 H$, M_i , K_i , and V_i denote the external field, saturation magnetization, anisotropy constant, and volume of the particle, respectively. Sub-index 1, 2 indicate the soft, hard region, respectively. J_e is the exchange constant and θ_i indicates the angle between the magnetic moments and the external field. In addition, demagnetizing energy was included properly in this model which was omitted by Suess et al. in their calculation [12]. The calculated results (see Fig. 5 (a) in Ref. [30]) show that the coercivity increases slowly with decreasing exchange coupling strength between the HL and SL in the strong coupling regime. As shown above by the VSM results, the investigated ECC films in this work are strongly coupled. With the increase of the Pt inter-layer thickness, the coupling strength is expected to decrease and then the small increase of the coercivity with the increase of the Pt inter-layer thickness can be understood naturally.

In order to prove that our exchange-coupled ECC media films are superior to the uncoupled films for perpendicular magnetic recording, we shall further examine the thermal stability of these films. Therefore, we measured the remnant coercivity $\mu_0 H_r$ of our films as a function of waiting time to study the magnetic decay behavior. The measurements were done as the following procedure: first, a negative field of 2 T was applied to saturate the sample, then the field was changed to positive ones near the coercive field for some waiting time t , after which the field was set to zero and the magnetization of the film were recorded. Then, the remnant coercivity $\mu_0 H_r(t)$ can be obtained by linear fitting of the measured $M(H)$ curve for every waiting time t . The thermal stability factor $K_u V/k_B T$ were evaluated by analyzing the time-dependent $\mu_0 H_r(t)$ using the Sharrock's equation [38],

$$H_r(t) = H_r(0) \left\{ 1 - \left[\frac{k_B T}{K_u V} \ln \left(\frac{f_0 t}{\ln 2} \right) \right]^{1/n} \right\}, \quad (2)$$

where f_0 is called the attempt frequency ($\sim 10^{10}$ Hz for magnetic systems [38]), $n = 1.5$ was fixed [39]. $K_u V$ is the energy barrier at zero applied field, and $k_B T$ is the thermal energy required to flip the magnetization.

The obtained thermal stability factor $K_u V/k_B T$ together with the coercivity are shown in Fig. 4 as a function of Pt inter-layer thickness for our ECC films. As can be seen, our uncoupled film has a stability factor of ~ 226 which is already much bigger than the typical values of the current perpendicular magnetic recording media using CoCrPt system ~ 80 [40]. Importantly, the stability factor for the ECC films have even bigger values of about ~ 600 . Similar to the FePt-C/FePt [5] system, the increased

thermal stability can be attributed to the increased switching volume due to the strong exchange coupling between the HL and SL. Therefore, our ECC media exhibit very good thermal stability and writability properties than the CoCrPt perpendicular magnetic recording system. Despite these interesting properties, when compared with other ECC systems using SLs with positive MA, there are relatively small amount of research works to study the ECC media films using SLs with negative MA. We expect that our work will promote further experimental and theoretical works to further improve the writability and other properties of the ECC media for high density magnetic recording.

4 Summary

In summary, we have grown and characterized $\text{Co}_{72}\text{Pt}_{28}/\text{Pt}(t\text{ nm})/\text{Co}_{81}\text{Ir}_{19}$ ECC media films with negative SL MA. TEM images show the columnar type growth of these ECC media films. Perfect c-plane oriented growth of these films have been evidenced by both TEM and XRD results. Single-step magnetization reversal process has been observed for our ECC media films, suggesting strong coupling between the hard and soft magnetic layers. More interestingly, our ECC media films exhibit much lower coercivities and much higher thermal stabilities than the uncoupled film which means that they are better suitable for high density perpendicular magnetic recording. These results are consistent with Victora's model and we expect that our work will simulate more experiments to further improve the magnetic properties of the ECC media with negative SL MA.

Funding Information This work was supported by the National Natural Science Foundations of China (Nos. 11704167 and 11574122) and the Fundamental Research Funds for the Central Universities (Nos. lzujbky-2017-k20 and lzujbky-2017-31).

References

1. Kanai, Y., Matsubara, R., Watanabe, H., Muraoka, H., Nakamura, Y.: IEEE Trans. Magn. **39**, 1955 (2003)
2. Suess, D., Schrefl, T., Fähler, S., Kirschner, M., Hrkac, G., Dorfbauer, F., Fidler, J.: Appl. Phys. Lett. **87**, 012504 (2005)
3. Suess, D.: Appl. Phys. Lett. **89**, 113105 (2006)
4. Victora, R.H., Shen, X.: Proc. IEEE **96**, 1799 (2008)
5. Wang, J., Sepehri-Amin, H., Takahashi, Y., Okamoto, S., Kasai, S., Kim, J., Schrefl, T., Hono, K.: Acta Mater. **111**, 47 (2016)
6. Varaprasad, B.S.D.C.S., Chen, M., Takahashi, Y.K., Hono, K.: IEEE Trans. Magn. **49**, 718 (2013)
7. Lu, L., Wu, M., Mallory, M., Bertero, G., Srinivasan, K., Acharya, R., Schulthei, H., Hoffmann, A.: Appl. Phys. Lett. **103**, 042413 (2013)
8. Takahashi, Y.K., Medapalli, R., Kasai, S., Wang, J., Ishioka, K., Wee, S.H., Hellwig, O., Hono, K., Fullerton, E.E.: Phys. R.V. Appl. **6**, 054004 (2016)

9. Suess, D., Schrefl, T., Dittrich, R., Kirschner, M., Dorfbauer, F., Hrkac, G., Fidler, J.: *J. Magn. Magn. Mater.* **551**, 290–291 (2005)
10. Berger, A., Supper, N., Ikeda, Y., Lengsfeld, B., Moser, A., Fullerton, E.: *Appl. Phys. Lett.* **93**, 122502 (2008)
11. Dobin, A.Y., Richter, H.: *Appl. Phys. Lett.* **89**, 062512 (2006)
12. Suess, D., Lee, J., Fidler, J., Schrefl, T.: *J. Magn. Magn. Mater.* **321**, 545 (2009)
13. Wang, Y., Li, F.S., Ariake, J., Honda, N., Ishio, S., Ouchi, K.: *J. Magn. Magn. Mater.* **320**, 3083 (2008)
14. Si, W., Zhao, G., Ran, N., Peng, Y., Morvan, F., Wan, X.: *Sci. Rep.* **5**, 16212 (2015)
15. Richter, H., Dobin, A.Y.: *J. Appl. Phys.* **99**, 08Q905 (2006)
16. Ghidini, M., Asti, G., Pellicelli, R., Pernechele, C., Solzi, M.: *J. Magn. Magn. Mater.* **316**, 159 (2007)
17. Livshitz, B., Inomata, A., Neal Bertram, H., Lomakin, V.: *Appl. Phys. Lett.* **91**, 182502 (2007)
18. Mukherjee, S., Berger, L.: *J. Appl. Phys.* **99**, 08Q909 (2006)
19. Sun, C.-J., Stafford, D., Acharya, R.: *IEEE Trans. Magn.* **46**, 1795 (2010)
20. Wang, F., Xu, X., Liang, Y., Zhang, J., Wu, H.: *Appl. Phys. Lett.* **95**, 022516 (2009)
21. Tsai, J.-L., Tzeng, H.-T., Lin, G.-B.: *Appl. Phys. Lett.* **96**, 032505 (2010)
22. Guo, H., Liao, J., Ma, B., Zhang, Z., Jin, Q., Wang, H., Wang, J.: *Appl. Phys. Lett.* **100**, 142406 (2012)
23. Xu, Z., Zhou, S., Ge, J., Du, J., Sun, L.: *J. Appl. Phys.* **105**, 123903 (2009)
24. Guo, H.H., Liao, J.L., Ma, B., Zhang, Z.Z., Jin, Q.Y., Rui, W.B., Du, J., Wang, H., Wang, J.P.: *J. Appl. Phys.* **111**, 103916 (2012)
25. Pandey, K., Chen, J., Chow, G., Hu, J.: *Appl. Phys. Lett.* **94**, 232502 (2009)
26. Saravanan, P., Hsu, J.-H., Tsai, C., Tsai, C., Lin, Y., Kuo, C., Wu, J.-C., Lee, C.-M.: *J. Appl. Phys.* **115**, 243905 (2014)
27. Pandey, K., Chen, J., Chow, G., Hu, J., Lim, B.: *J. Appl. Phys.* **105**, 07B733 (2009)
28. Tang, R., Chua, S., Zhang, W., Li, Y.: *J. Magn. Magn. Mater.* **323**, 2569 (2011)
29. Girt, E., Dobin, A.Y., Valcu, B., Richter, H., Wu, X., Nolan, T.P.: *IEEE Trans. Magn.* **43**, 2166 (2007)
30. Jiao, J.Y., Ma, T.Y., Li, Z.W., Qiao, L., Wang, Y., Wang, T., Li, F.S.: *J. Phys. D: Appl. Phys.* **51**, 055007 (2018)
31. Victora, R.H., Shen, X.: *IEEE Trans. Magn.* **41**, 537 (2005)
32. Xu, F., Wang, T., Ma, T., Wang, Y., Zhu, S., Li, F.: *Sci. Rep.* **6**, 20140 (2016)
33. Ma, T., Jiao, J., Li, Z., Qiao, L., Wang, T., Li, F.: *J. Magn. Magn. Mater.* **444**, 119 (2017)
34. Pandey, K., Chen, J., Lim, B., Chow, G.: *J. Appl. Phys.* **104**, 073904 (2008)
35. Mukai, R., Uzumaki, T., Tanaka, A.: In: INTERMAG 2006 - IEEE International Magnetism Conference, pp. 12–12 (2006)
36. Jiao, J., Wang, T., Ma, T., Wang, Y., Li, F.: *Nanoscale Res. Lett.* **12**, 21 (2017)
37. Pandey, K.K.M., Chen, J., Chow, G.: *J. Appl. Phys.* **100**, 054909 (2006)
38. Sharrock, M.P.: *J. Appl. Phys.* **76**, 6413 (1994)
39. Suess, D., Eder, S., Lee, J., Dittrich, R., Fidler, J., Harrell, J.W., Schrefl, T., Hrkac, G., Schabes, M., Supper, N., et al.: *Phys. Rev. B* **75**, 174430 (2007)
40. Piramanayagam, S.N.: *J. Appl. Phys.* **102**, 011301 (2007)